Seismic reflection and transmission within an extended scatterer

Kris Innanen

ABSTRACT

A range of methods for making FWI stable in its construction of long wavelength model components in deep regions of the model (relative to maximum offset) have been introduced over the last several years, as discussed and presented by Geng, Almuteri and Innanen in CREWES. Many of these either quantitatively or qualitatively invoke multiple scattering. Using multiple scattering formalisms to model wave fields is not straightforward when the model error or perturbation is large, however. In this paper a Matlab code that quickly models the nth order truncated Born series approximation of a 1D wave field is written and used to flesh out some of the ways the series goes about creating events like direct arrivals and coda contributions. The main conclusion is a reminder not to say things like "the series did not converge by Nth order", but only things like "the series only converged to a maximum frequency f_n by nth order".

INTRODUCTION

A range of seismic waveform inversion methodologies have emerged recently which work towards reconstructing regions of the model for whom offset/depth ≈ 1. This is difficult to accomplish with normal FWI. Standard FWI kernels, which are, roughly speaking, the basis functions out of which the model update is constructed, only contribute to the long-wavelength parts of the model at very limited depths (see Figure 1, left panel). These kernels are activated by long-offset direct arrivals. If the background medium has a velocity trend, these kernels dive into deeper regions and then turn back up, but that penetration is always quite limited. Reflection data activate kernels also, and these can constrain the deeper parts of the model, but, from a classical result of diffraction tomography (Devaney, 1982), we know that reflection modes only constrain short-wavelength model components.

In response to this, reflection FWI (for a comprehensive review, see the recent thesis of Almuteri, 2017), and a range of nonlinear FWI methods, by putting in place real or estimated scattering points in the deeper parts of the model, force new kernels to be activated, similar in character to the so-called "rabbit ears" of full wave imaging (see Figure 1, right panel). Convincing case studies have yet to be published, but these methods appear to have strong potential for increasing the depth of investigation and the convergence rate of FWI (e.g., Alkhalifah and Wu, 2016; Geng et al., 2017).

As we begin to consider incorporating multiple scattering into FWI kernels, especially in a truly nonlinear sense and when the model error or perturbations considered are large and sustained, some refreshers on the way multiple scattering actually goes about constructing wavefields is worthwhile.

Two statements are relatively common to hear in presentations on multiple scattering:

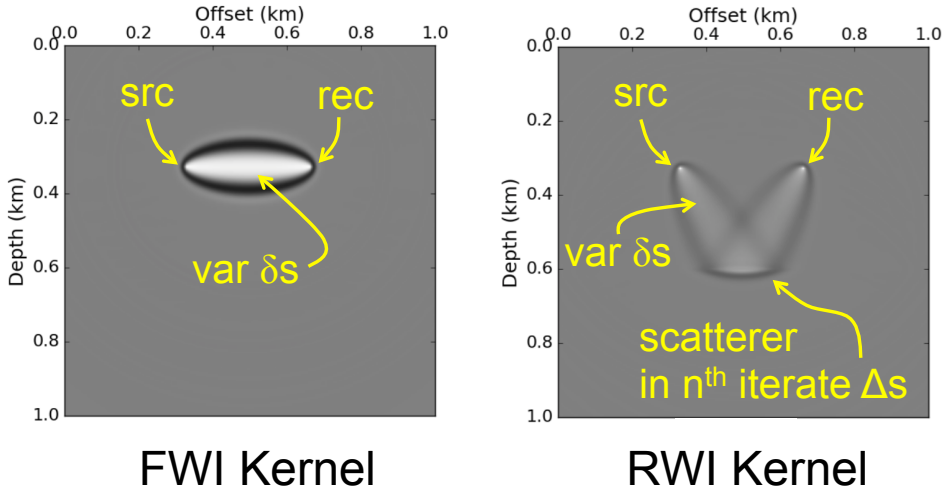

FIG. 1. Standard FWI kernels (left panel) versus reflection based full waveform inversion kernels (right panel). Kernels are built by scattering a wave, which is propagating from some source point to a receiver point in the background medium, from variation points throughout the model. Reflection FWI kernels (right panel) are in contrast built by scattering the wave that starts from the source, ends at the receiver, and scatters from a secondary target, at a variation point either before or after it hits the secondary target.

1. "The series was computed to nth order, but it did not converge."
2. "The nth order term in the series constructs the nth order event in the data."

Neither of these remarks is wrong, necessarily, but both deserve more complete statements. The purpose of this paper is to discuss what kinds of additional statements would help.

To generate numerical examples which will exemplify and justify our conclusions, a numerical framwork for 1D scalar ftruncated Born series approximations has been assembled; essentially the numerical version of the analytic system used by Matson (1996) to draw conclusions about various aspects of Born series behaviour. The mathematical formulation is set out, and a set of example 1D wavefield (i.e., trace) constructing forward modelling problems are solved.

FORMULATION

A series formula for a multiply-scattered wave in the Earth

Let the 1D wave ϕ propagate in a scalar acoustic Earth according to the equation

$$\left[\frac{d^2}{dz^2} + \frac{\omega^2}{c^2(z)}\right] \phi(z, z_s, \omega) = \delta(z_g - z_s). \tag{1}$$

If the medium $c(z)$ is decomposed into a homogeneous reference medium c_0 and a perturbation $a(z) = 1 - c_0^2/c^2(z)$, a scattering equation for ϕ of the form

$$\phi(z, z_s, \omega) = G(z, z_s, \omega) + k^2 \int_{-\infty}^{\infty} dz' G(z, z', \omega) a(z') \phi(z', z_s, \omega)$$

can be derived, where $k = \omega/c_0$ and G is

$$G(z, z_s, \omega) = (i2k)^{-1} \exp(ik|z - z_s|).$$

To enable later approximations, let us instead consider the field P satisfying

$$P(z, z_s, \omega) = G(z, z_s, \omega) + k^2 \int_{\alpha(z,z_s)}^{\beta(z,z_s)} dz' G(z, z', \omega) a(z') P(z', z_s, \omega), \tag{2}$$

in which we have formally introduced the limits α and β such that

$$\lim_{\alpha \to -\infty} \left(\lim_{\beta \to \infty} P \right) = \phi.$$

Equation (2) can be solved by expanding it in a Born series (e.g., Weglein et al., 2003). The terms of the series can furthermore be expressed recursively (Matson, 1996; Innanen, 2009), upon doing which the formula for the wave P at z caused by a source at z_s and having interacted with the medium $c(z)$ becomes

$$P(z, z_s, \omega) = \sum_{n=0}^{\infty} P_n(z, z_s, \omega), \tag{3}$$

where

$$P_n(z, z_s, \omega) = -\frac{ik}{2} \int_{\alpha(z,z_s)}^{\beta(z,z_s)} dz' \exp(ik|z - z'|) a(z') P_{n-1}(z', z_s, \omega) \tag{4}$$

and $P_0(z, z_s, \omega) = G(z, z_s, \omega)$.

Qualitative interpretation of equation (4)

The waveform P is computed in practice by summing a finite number of the terms P_n. From equation (3) we observe that each P_n appears as a relatively simple integral operation on the preceding series term P_{n-1}. In Figure 2 the qualitative interpretation of the term P_n is illustrated. In Figure 2a the source position, possible observation positions, and the reference field P_0 incident on the perturbed medium are illustrated. Scattering equations are always read from right to left. In Figures 2b-c the right-to-left reading of equation (4) is illustrated schematically. Each point in the perturbed region of the Earth is labelled with a z'. At nth order, the position z' is illuminated from above and below by the total field P_{n-1}; the incident field is weighted by the perturbation $a(z')$, and the result acts as a source in the reference medium which propagates directly to the observation point z. P_n is the superposition of these fields for each z'. For any n, as z' contributions are added, some will be "above" the measurement point, i.e., $z' < z$ (Figure 2b), and others will/may be "below", i.e., $z' > z$ (Figure 2c).

WKBJ as a special case

Summing different numbers of terms in equation (3), and allowing or disallowing contributions from certain scattering points z' (see Figure 2), all produce different approximations of P. To demonstrate this, consider equation (2) in the special case where

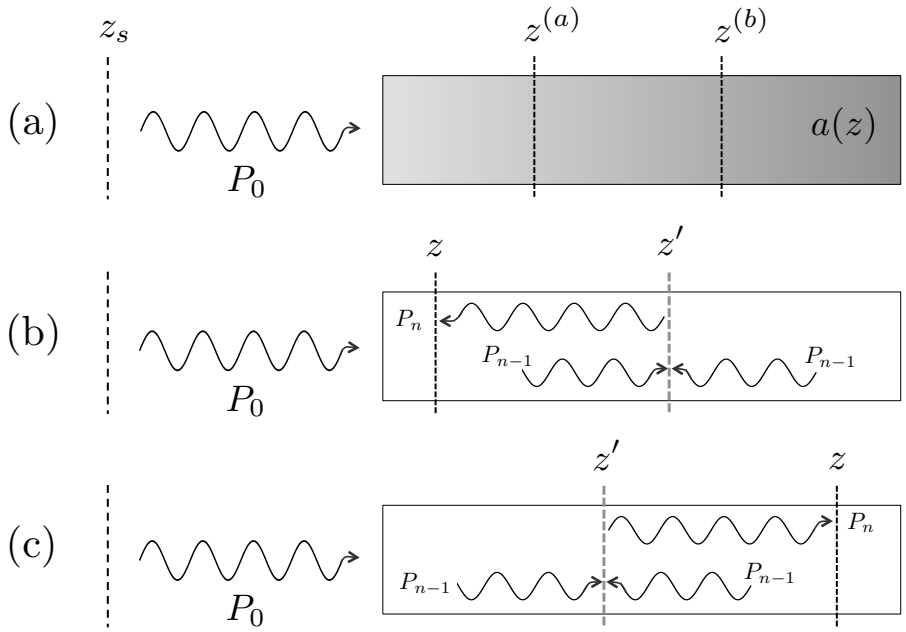

FIG. 2. Schematic representation of the multiple scattering formula. (a) A source wave P_0 is incident on a general perturbation $a(z)$, and the resultant field P observed at an arbitrary point (e.g., $z^{(a)}$ or $z^{(b)}$) is to be calculated. (b) Equations (3) – (4) represent the resultant field as the sum of contributions P_n at the observation point z. Each P_n is constructed as follows. A point z' is illuminated with the total up- and down-going field P_{n-1}, after which it is assigned a scattering amplitude proportional to $a(z')$, and it is propagated directly to the observation point z. The total response at z is the superposition of this influence for all z' between α and β for which $a \neq 0$.

$\alpha(z, z_s) = z_s$ and $\beta(z, z_s) = z$. Letting the field satisfying this integral equation be called T, we have

$$T(z, z_s, \omega) = (i2k)^{-1} e^{ik(z-z_s)} + -\frac{ik}{2} \int_{z_s}^{z} dz' e^{ik(z-z')} a(z') T(z', z_s, \omega). \tag{5}$$

This equation is used by Morse and Feshbach (1953) for the derivation of the WKBJ approximation. Multiplying by e^{ikz} and applying d/dz, we obtain a new differential equation in T, simpler than that of equation (1):

$$\frac{dT(z, z_s, \omega)}{dz} = ik \left(1 - \frac{1}{2} a(z)\right) T(z, z_s, \omega),$$

which can be directly integrated to produce

$$T(z, z_s, \omega) = T_0 \exp\left[ik \left(1 - \frac{1}{2} \int_{z_s}^{z} a(z') dz'\right)\right], \tag{6}$$

with T_0 to be determined. Equation (7) is the WKBJ approximation — a one-way wave whose travel time is determined by the integral of the velocity structure between z_s and z. This is a rather dramatic simplification of the two-way waveform P which, when rendered exactly, can have any number of coda events.

How did we suppress this much of the wave? By choosing a value for $\beta(z, z_s)$ that suppresses all contributions from depths z greater than the observation point. Specifically,

by allowing contributions like Figure 2b and disallowing contributions like Figure 2c. Evidently, these scattering contributions coming from above the measurement point construct the most important part of the wave, but, if we consider reflections and reverberations happening within the structure $c(z)$ to be important, retaining at least some of the deeper contributions will be necessary.

An algorithm for multiply-scattered waveform modelling

Computing discrete versions of equations (3)–(4) in which $\beta \to \infty$ will evidently produce several important components of the waveform that are lost when the WKBJ approximation is made. However, this requires that we incorporate repeated extended integrations over (potentially) quite large intervals of depth, and make the endpoint or maximum depth distant enough that an artificial reflection from it does not interfere with the simulated waveform. Intuitively it seems unlikely that a point far remote from, and below, a set of contributing structures and an observation point could have a large impact on the wave. Furthermore the integral of the full perturbation included in the calculation affects convergence and convergence rate, as we shall demonstrate, so if this contributing integral can be shrunk without affecting the result so much the better. Thus we attempt a compromise, computing iteratively the following quantity:

$$\Phi(z, z_s, \omega) = \sum_{n=0}^{\infty} \Phi_n(z, z_s, \omega), \tag{7}$$

where

$$\Phi_n(z, z_s, \omega) = -\frac{ik}{2} \int_{z_s}^{\mathrm{Z}} dz' e^{if(z,z',\lambda)} a(z') \Phi_{n-1}(z', z_s, \omega), \tag{8}$$

and

$$f(z, z', \lambda, \Delta z) = \begin{cases} ik(z - z') & z' < z, \\ ik(z' - z), & z < z' < z + \Delta z \\ ik(z' - z)(1 + i\lambda), & z + \Delta z < z' \end{cases} . \tag{9}$$

where λ is a small positive constant. This invokes a non-physical (non-dispersive) wave absorption for all contributions coming from scattering points z' below the current output point.

NUMERICAL CONVERGENCE

A Matlab code was written to explore the algorithm in equations (7)-(9), with the output analyzable in both the frequency and time domains, with a general perturbation $a(z)$ away from the reference c_0, variable receiver location, and variable bandwidth. The model in Figure 3 is used for creating all numerical examples to follow.

Restricted series for direct wave

First let us see that the restricted series that is consistent after convergence with the WKBJ approximation, and which therefore can only be involved with the construction

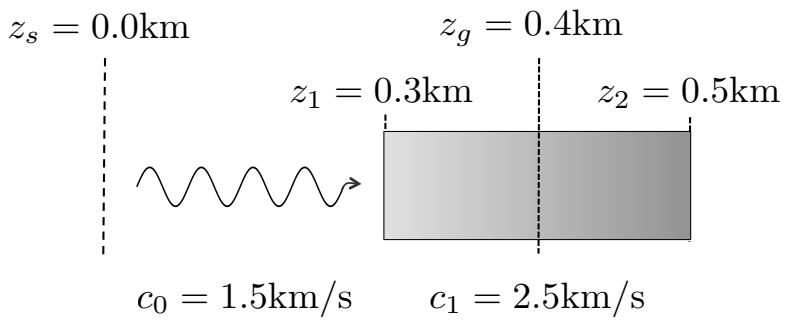

FIG. 3. Model used for all numerical examples to follow.

of the zero'th order event in a data set (i.e., the direct arrival), requires many orders of scattering to create a numerically meaningful approximate solution. This is the numerical justification for the statement that, when model error / perturbations are large and extended, "all orders of scattering are needed to compute each order of event".

A convergent instance of the WKBJ series is illustrated in Figure 4. In the left panel, the 0th order term as calculated on the backdrop of the model in Figure 3 is plotted. Evidently it creates a 0th order event, the direct arrival, but this event can be observed to be in error relative to the expected arrival time and amplitude of the event (blue solid and dashed lines respectively). In the right panel, the field approximated with 20 terms is plotted.

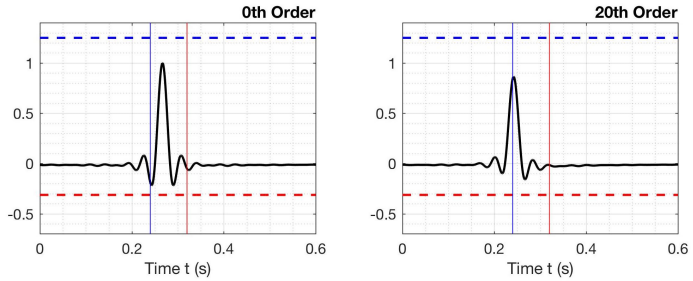

FIG. 4. A convergent instance of the algorithm in equations (7)-(9). Parameters: c_0=1.5km/s, c_1=2.5km/s; corner frequencies (0,1,25,35)Hz; src/rec positions 0.0km / 3.5km, interface positions 3.0km, 5.0km. Left panel: 0th order approximation, right panel: 20th order approximation.

Notice that (1) the arrival time of the 0th order event is largely corrected, but (2) its amplitude is not, and (3) it has some minor phase alterations; also (4) no part of the coda, e.g., the expected reflection at time/amplitude given by the red solid and dashed lines, appears. These four properties are consistent with the WKBJ approximation. Evidently we must dispense with the qualitative / mnemonic idea that nth order scattering and nth order events are necessarily one-to-one concepts.

How should we think of the multiple scattering, order by order, construction of a field when the perturbation is large and extended? One useful mental image is the Maclaurin series construction of a simple function, such as e^{-x}. Suppose we used the series

$$e^{-x} = 1 - x + \frac{1}{2}x^2 - \frac{1}{6}x^3 + ..., \tag{10}$$

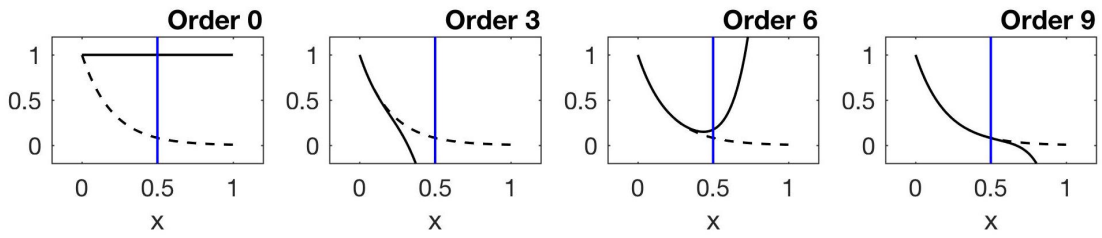

FIG. 5. Characteristics of a truncated Maclaurin series approximation of e^{-x} over a range of x values. As terms are added, the approximation "has converged" over a broader x interval. At any truncation order it is incomplete to say that the series has or has not converged; rather the series has or has not converged over a given x interval at that order.

to create a set of approximations of e^{-x} over a fixed x interval, say $(0, 1)$. The series is known to converge for all possible x. But, how does it happen? Figure 5 shows some example truncation orders. Evidently what happens is, the function converges over an increasing range of x values as terms are added. It converges at $x = 0$ immediately, and by the time we have reached order 8, it appears to have largely converged on the interval $(0, 0.5)$.

The Born series is acting this way, more or less, but in the construction of quantities like $e^{i(2\pi\tau_0)f}$, for a fixed arrival time, over a range of f. That is, as we add orders, we create a convergent wave field approximation over a growing range of frequencies f starting with 0.

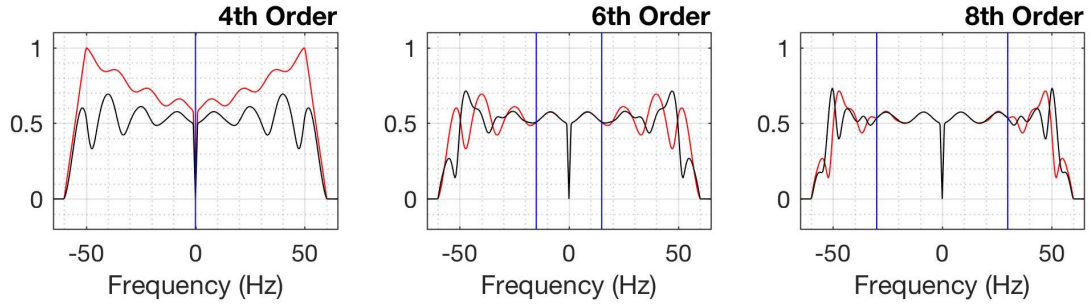

FIG. 6. Three approximations of the WKBJ field at different truncation orders: 4th, 6th, 8th. Current approximation is plotted in black, previous order in red. Blue lines indicate the points along the f axis at and below which the series has converged.

In Figure 6, the 4th, 6th and 8th order approximations of the WKBJ field is plotted in the frequency domain (black), alongside the previous order (red). Regions where the black and red curves match we conclude the series has largely converged. The frequency band of convergence grows from 15 to 30Hz as we move from 6th to 8th order. *If you compute n series terms, it is incomplete to say "the series did not converge"; it is only complete to say, "the series did not converge over the frequency band* $(0, f_n)$*".*

Time-domain convergence for two different bands

More often than not truncated versions of the series are observed for convergence in the physical (time) domain rather than the frequency domain. Returning to Figure 5, we

may predict the result of such an examination. If the series has converged over a band that has a lower maximum than the band of frequencies used to make the time domain approximation, the spectrum of the approximate field will have the features of the 6th order panel in the figure. Namely, although it will have converged over a fair range, beyond that range it will grow rapidly and without bound. If we were to inverse Fourier transform this approximation, the result would therefore oscillate rapidly and at extremely high amplitude.

Figures 7-10 illustrate this. By the 20th order the approximation has settled down and largely converged, but prior to this order it appears to oscillate rapidly. Although it eventually converges, this manner of examination of the series convergence is not particularly instructive. At order 10 (Figure 8), the approximation appears to be wildly inaccurate and of little value; however, inspection of the spectrum at order 8 in Figure 6 reminds us that over a different frequency band (this example has a maximum frequency of 45Hz), a fully converged result has already been obtained.

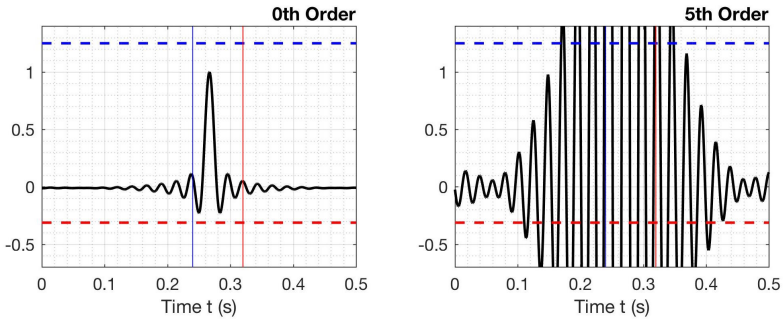

FIG. 7. Convergence and bandwidth. Ormsby parameters 0Hz-1Hz-40Hz-45Hz. Series is truncated at order 5.

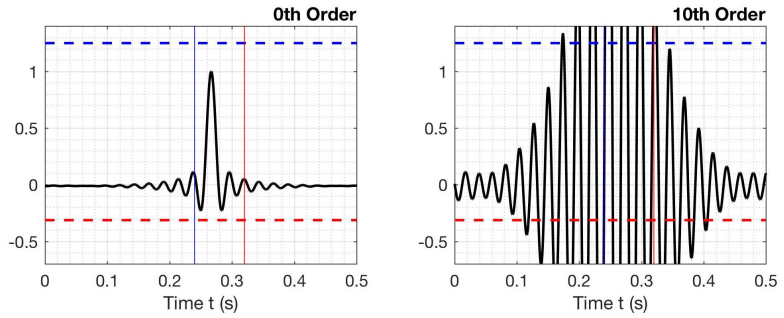

FIG. 8. Convergence and bandwidth. Ormsby parameters 0Hz-1Hz-40Hz-45Hz. Series is truncated at order 10.

We see this by trying the time-domain experiment again, but this time for the approximation of the WKBJ field with a maximum frequency of 25Hz rather than 45Hz. The same orders are plotted in Figures 11-14. Consider again the 10th order approximation. This time it has "settled down" significantly, and in fact undergoes little observable change over the remaining 10 orders examined.

Thus, it is quite misleading to pass judgment on the convergence of a Born series multiple scattering wave field approximation at a given order by examining its time-domain form. If this is to be done, it should be done by filtering the spectrum beyond the conver-

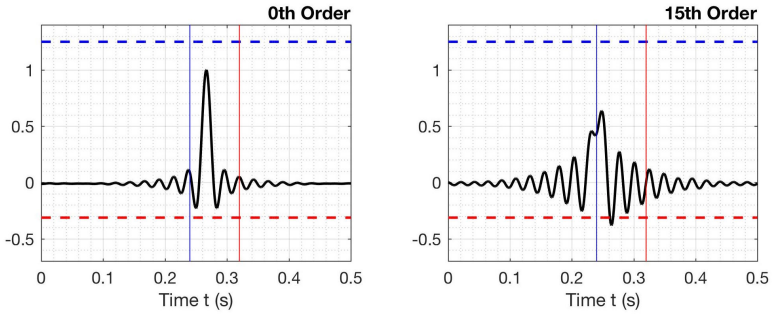

FIG. 9. Convergence and bandwidth. Ormsby parameters 0Hz-1Hz-40Hz-45Hz. Series is truncated at order 15.

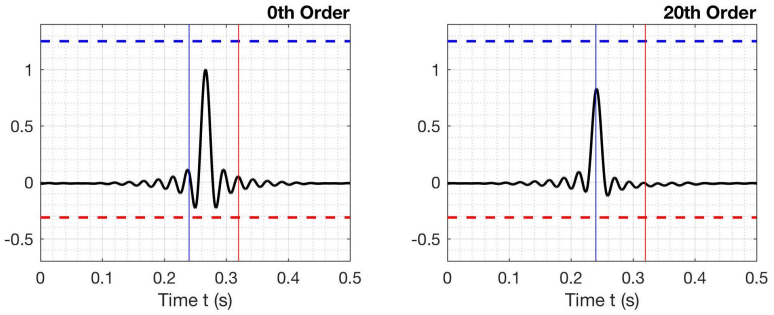

FIG. 10. Convergence and bandwidth. Ormsby parameters 0Hz-1Hz-40Hz-45Hz. Series is truncated at order 20.

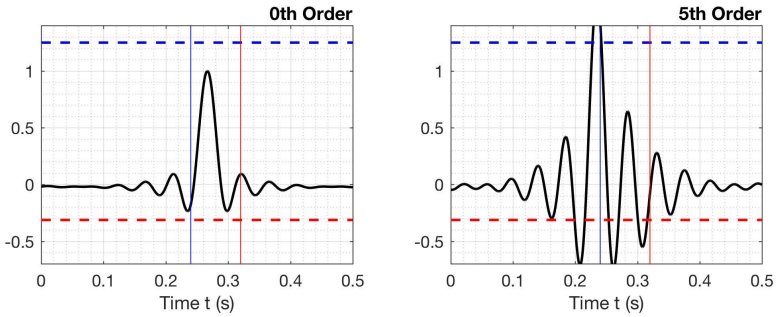

FIG. 11. Convergence and bandwidth. Ormsby parameters 0Hz-1Hz-20Hz-25Hz. Series is truncated at order 5.

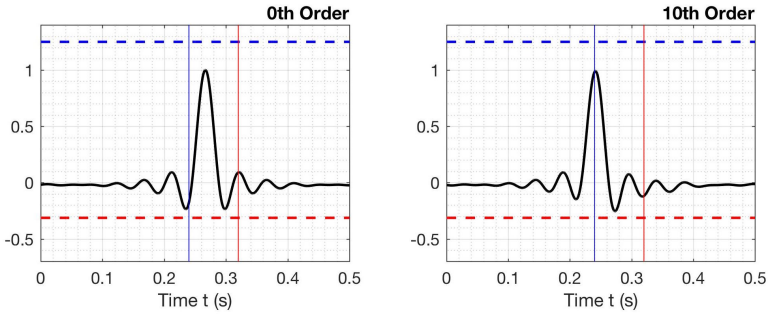

FIG. 12. Convergence and bandwidth. Ormsby parameters 0Hz-1Hz-20Hz-25Hz. Series is truncated at order 10.

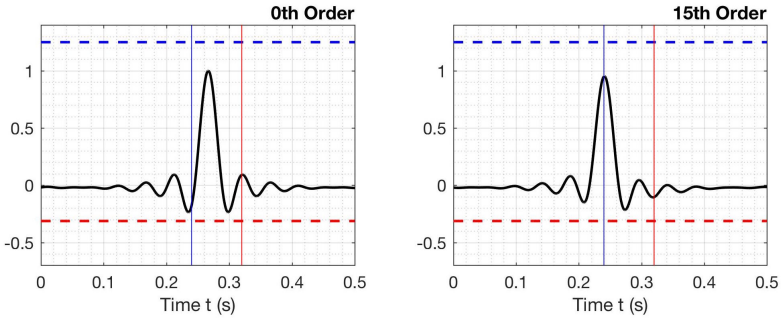

FIG. 13. Convergence and bandwidth. Ormsby parameters 0Hz-1Hz-20Hz-25Hz. Series is truncated at order 15.

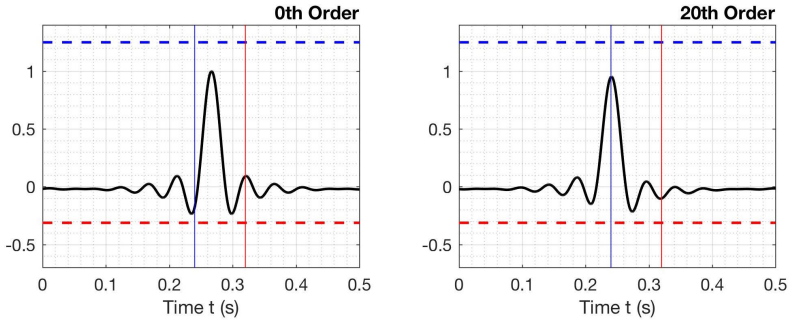

FIG. 14. Convergence and bandwidth. Ormsby parameters 0Hz-1Hz-20Hz-25Hz. Series is truncated at order 20.

gence frequency. An nth order Born series approximation can be criticized for its bandwidth, but not its rapid oscillations.

Full scattering and coda waveforms

Removing the restriction on scattering geometry changes the character of the series and makes convergence much more difficult to discuss and predict. Numerical examples are strongly suggestive that there remain bandwidths over which the field caused by almost any perturbation stably converges, but the author sees little in the way of predictable pattern, beyond, "bigger" perturbations mean lower-frequency convergence bands.

Nevertheless, it is worth noting for those considering incorporating multiple scattering in sensitivity kernel construction, that coda waves and reflections can be stably and accurately produced.

In Figure 15, the 0th, 4th and 10th order approximations of the wavefield, generated for the source/receiver and model configuration illustrated in Figure 3, for full scattering $\beta \rightarrow \infty$ are plotted. The correct construction of the reflection from the z_2 interface back up to the receiver is clearly visible.

CONCLUSIONS

Multiple scattering can be accurately modelled using numerical integration and formalisms derived from the Born series. These computations, especially in 3D, can be quite

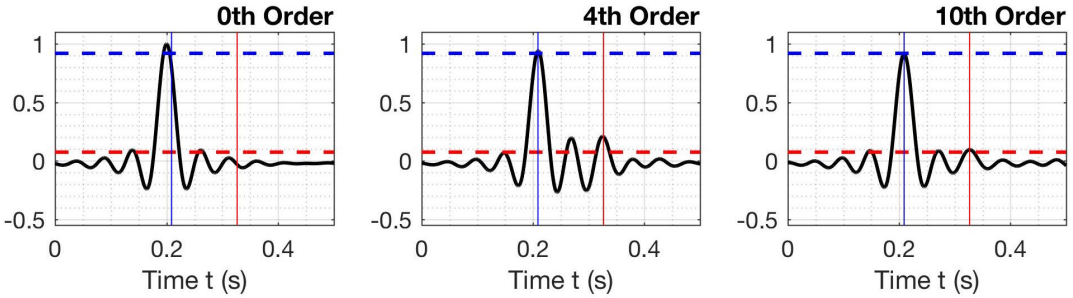

FIG. 15. Full series for constant perturbation. Reflection / coda now visible; amplitudes of direct and transmitted waves accurate.

laborious, but many of the apparently disappointing features of a first attempt at numerical simulation of waves with truncated series expansions (wherein the series appears to oscillate wildly and diverge) are actually easily remedied figments.

This may have important consequences for research groups (like ours) who are interested in bolstering FWI kernels with robust, "depth-resolving" multiple scattering kernels that nonlinearly invoke multiple scattering and which are "aware" that the model perturbations are not pointlike or small.

When analyzing the numerical results of a truncated series expansion of a wavefield, it is inaccurate or at least incomplete, to claim that the series did not converge. It is much more helpful and accurate to claim that it did not converge over a particular frequency band. Better yet, the approximation should be analyzed in both the frequency and time domains, with the time domain version filtered so that the high frequency polynomial component of the approximation, which does not carry any useful information, is suppressed.

ACKNOWLEDGEMENTS

We thank the sponsors of CREWES for continued support. This work was funded by CREWES industrial sponsors and NSERC (Natural Science and Engineering Research Council of Canada) through the grant CRDPJ 461179-13.

REFERENCES

Alkhalifah, T., and Wu, Z. D., 2016, Multiscattering inversion for low-model wavenumbers: Geophysics, **81**, No. 6, R417–R428.

Almuteri, K., 2017, Evaluating the potential of reflection-based waveform inversion, MSc Thesis, University of Calgary.

Devaney, A. J., 1982, A filtered backpropagation algorithm for diffraction tomography: Ultrasonic Imaging, **4**, No. 4, 336–350.

Geng, Y., Pan, W., and Innanen, K. A., 2017, Frequency-domain full-waveform inversion with nonlinear descent directions: Submitted to: Geophysical Journal International.

Innanen, K. A., 2009, Born series forward modeling of seismic primary and multiple reflections: an inverse scattering shortcut: Geophys. J. Int., **177**, No. 3, 1197–1204.

Matson, K. H., 1996, The relationship between scattering theory and the primaries and multiples of reflection seismic data: Journal of Seismic Exploration, **5**, 63–78.

Morse, P. M., and Feshbach, H., 1953, Methods of theoretical physics: McGraw-Hill Book Co.

Weglein, A. B., Araújo, F. V., Carvalho, P. M., Stolt, R. H., Matson, K. H., Coates, R. T., Corrigan, D., Foster, D. J., Shaw, S. A., and Zhang, H., 2003, Inverse scattering series and seismic exploration: Inverse Problems, , No. 19, R27–R83.